Dependence of solid particle erosion on the cross-link density in an epoxy resin modified by hygrothermally decomposed polyurethane

N.-M. Barkoula, J. Gremmels, J. Karger-Kocsis*

Institute for Composite Materials Ltd., University of Kaiserslautern,
P.O. Box 3049, D-67653 Kaiserslautern, Germany

Abstract

Solid particle erosion of epoxy resin (EP) modified by various amounts of hygrothermally decomposed polyester-urethane (HD-PUR) was studied at oblique (30, 45, and 60°) and normal impact (90°). The cross-linked structure of the modified EP was characterised by the mean molecular weight between cross-links (M_c). It was established that the initial brittle erosion of the densely cross-linked EPs ($M_c \leq 200$ g/mol) changed to a rubbery one by increasing HD-PUR modification due to which a less cross-linked network was formed ($M_c > 1000$ g/mol). This change was reflected by the impact angle dependence: compositions of low M_c showed the minimum resistance at normal (90°), whereas those of high M_c at 30° impact angle. The resistance to solid particle erosion changed linearly with increasing fracture energy (G_c) of the resins. G_c, on the other hand, followed the prediction of the rubber elasticity theory and increased linearly with $M_c^{1/2}$. © 2001 Elsevier Science B.V. All rights reserved.

Keywords: Modified epoxy resin (EP); Solid particle erosion; Cross-link density; Fracture energy; Failure behaviour

1. Introduction

Polymers and related composites are widely used as engineering parts in various application fields where high resistance to wear, abrasion and erosion is required (mining, energetics, transportation, etc.) [1]. As a consequence, the erosion wear performance of polymeric systems became under spot of interest recently. Albeit polymers and related composites possess outstanding mechanical and thermal properties, many of them show rather poor resistance when exposed to fast moving erodents [2]. The latter occurs very frequently in the praxis. The erosion behaviour of polymeric materials depends first of all on their nature. Thermosetting polymers, such as epoxy (EP) and phenolic resins, show brittle erosion whereas the erosion response of thermoplastics is of ductile type [3]. The same categorisation applies for the related composites. It was demonstrated that the maximum erosion rate is at an oblique impact angle of 30° and at 60–90° for ductilety and brittely eroding polymers, respectively [1,3–7]. Rubbers, on the other hand, present a

maximum erosion rate at 30°, but the failure mechanisms differ from those of thermoplastic resins.

It is, therefore, a great challenge to study the solid particle erosion of a system that may show both brittle and ductile erosion behaviour depending on its composition and structural characteristics. According to the authors knowledge this has not been done so far. Recently, it was reported that the mechanical property profile of tri-and tetrafunctional EP resins can be varied in a very broad range by modifying them with hygrothermally decomposed polyester-urethane (HD-PUR) [8,9]. HD-PUR works as an active diluent (being an amine containing compound) and phase separation modifier at the same time in EP resins. The properties of the EP/HD-PUR systems can be set between those of cross-linked thermosets and rubbers via the HD-PUR amount. Modification of EP by HD-PUR results in a chemical network of lower cross-link density. This fact allows us to investigate the erosive behaviour as a function of network characteristics. The aim of this study was to investigate the effects of external testing conditions (impact angle) and internal material parameters (cross-link density) on the erosion behaviour of HD-PUR modified EP resins. A further aim of this study was to find a correlation between

* Corresponding author.
E-mail address: karger@ivw.uni-kl.de (J. Karger-Kocsis).

Table 1
Designation and composition of the EP resins studied

Designation	HD-PUR (wt.%)	Hygrothermal decomposition in presence of glycine	Hardener (DDS: 33 wt.%)
EP	0	–	+
EP/HD-PUR-G	10, 20, 40, 60, 80	+	+
EP/HD-PUR	60, 80	–	+
EP/HD-PUR-G*	33	+	–
EP/HD-PUR*	33	–	–

the erosion resistance and the fracture mechanical response of the modified EPs.

2. Experimental

2.1. Materials and their characteristics

Table 1 lists the composition and designation of the EP materials tested. In the present study nine modifications in addition to the pure EP were investigated.

The hygrothermal decomposition of polyurethane (HD-PUR) along with its characteristics and the way of EP modification were described in our earlier papers [8,9]. Briefly, polyester-based PUR processing waste was ground to a particle size of 1–3 mm. To these PUR particles 10 wt.% of water, sometimes as a solution with coagent (glycine, G) was added and fed in the hopper of a laboratory-scale twin screw extruder in which the hygrothermal decomposition of PUR was performed. The HD-PUR produced for this study was decomposed at $230°C$ and its acetone insoluble fraction was 14 wt.%.

A trifunctional EP resin (MY 0500, Ciba) was mixed with 10–80 wt.% HD-PUR. The EP/HD-PUR mixtures were homogenised by careful stirring before the hardener, diaminodiphenylsulphone (DDS; HT 976, Ciba) was introduced in 33 wt.% and mixed again. As HD-PUR is an amine-rich compound it can replace the DDS, which was practised in some formulation (i.e. HD-PUR was added in 33 wt.%) for the sake of comparison. The whole procedure of the preparation of the materials was described in our previous works [8,9]. The mean molecular weight between cross-links (M_c)

was computed from the rubbery plateau modulus (E_R) determined by dynamic-mechanical thermoanalysis (DMTA). The DMTA tests were conducted on an Eplexor^{TM} 150 N (Gabo Qualimeter). Viscoelastic material parameters such as mechanical loss factor and complex tensile Young's modulus (tan δ and E^*, respectively) were measured in tensile loading over a broad temperature range (-100 to $+300°C$) at a heating rate of $0.6°C/min$ at a frequency of 10 Hz. The M_c data are listed in Table 2. It should be mentioned here, that M_c could not be easy determined for the EP resins with low HD-PUR content due to their starting thermal decomposition. Therefore, E_R was read from the intersection of the slopes related to the T_g step and onset of the rubbery plateau of the E^* versus T traces [8]. Further, the M_c data in Table 2 were derived from one single DMTA spectrum for each composition. This is the reason of some anomalies with respect to the M_c data in Table 2.

For the fracture mechanical characterisation of the samples compact tension (CT) specimens were used. They were cut from plates produced in Teflon^{TM} molds. The saw-induced notch of the CT-specimens was sharpened by a razor blade prior to their loading at 1 mm/min deformation rate at room temperature (RT). The fracture toughness (K_c) and fracture energy (G_c) were determined according to the ESIS testing protocol [10]. The hardness of the compositions was assessed by Shore values on a Zwick 3114 hardness tester (DIN 53 505).

2.2. Solid particle erosion

All erosion tests were performed in a sand-blasting chamber using sharp angular corundum particles with a size

Table 2
Change in the hardness, fracture mechanical (K_c, G_c); DMTA (T_g, E_R) and cross-link (M_c) parameters as a function of type and amount of HD-PUR

PUR (wt.%)	EP/HD-PUR						EP/HD-PUR-G					
	Shore A or D	K_c (MPa m$^{1/2}$)	G_c (kJ/m^2)	T_g (°C)	E_R (MPa)	M_c (g/mol)	Shore A or D	K_c (MPa m$^{1/2}$)	G_c (kJ/m^2)	T_g (°C)	E_R (MPa)	M_c (g/mol)
0	85-D	0.61	0.25	260	116.8	173	85-D	0.61	0.25	260	116.8	173
10	85-D	0.98	0.62	250	101.2	171	85-D	0.94	0.54	240	114.5	149
20	85-D	0.72	0.32	207	111.33	145	85-D	1.07	0.8	205	79.2	205
33 (no hardener)	75-D	–	–	45	–	877	75-D	1.2	0.70	75	–	537
40	80-D	1.66	1.54	140	43.8	309	80-D	1.41	1.1	140	27.6	506
60	68-D	1.35	3.15	80	11.0	1114	68-D	1.19	2.37	80	12.6	938
80	80-A	–	–	40	8.4	1067	75-A	–	–	40	4.6	2082

between 60 and 120 μm. The distance between the sampler holder and the nozzle was constant (220 mm). The eroded area was kept constant through a steel cover frame with circular opening which was positioned on the surface of the specimens. The impact angle was adjusted by turning the sample holder. The speed of the erodent particles was kept constant ($\cong$70 m/s) by setting 6 bar air pressure in the nozzle. All erosion test were performed at RT.

The mass loss of the modified EPs was recorded as a function of erosion time by a precision balance (AT261 Mettler Toledo; sensibility 50 μg). There was no corundum particles on the specimen surface, as they were removed after every erosion impact by air blasting.

As mentioned above, the material removal caused by jet-erosion is grouped into rubbery, ductile and brittle one. The mass loss versus time diagrams of the EPs corroborated the existence of these types of erosion. In ductile and rubbery type of erosion, an incubation period could also be found.

Four impingement angles were selected (30, 45, 60, and 90°) in order to obtain a clear view in respect to the transition between the two types of erosion as the HD-PUR content was increased in the EP resins.

The eroded surfaces of some selected specimens were inspected in a Jeol scanning electron microscope (SEM) in order to conclude the erosion mechanisms. The samples were gold-sputtered to reduce electrostatic charging of the surface.

3. Results and discussion

3.1. Cross-linked network structure

Fig. 1 presents the variation of the glass transition temperature (T_g) and rubbery plateau modulus (E_R) values as a function of HD-PUR-G amount, as read from DMTA spectra [8].

One can notice that the T_g shifts towards lower temperatures with increasing amount of the modifier. E_R also reduced while increasing modifier content. This implies that the HD-PUR and HD-PUR-G participate in the formation of the cross-linked network structure and consequently, they work as an active diluent (plasticizer) in EP. All these findings are based on the fact that the hydrolytic decomposition of PUR provides a primary amine-rich rubbery compound [8,9]. A detailed analysis of the change in T_g and E_R as a function of the modifier type and content showed that HD-PUR is involved in the formation of both cross-linked EP network and a disperse phase therein [8,9]. Considering the E_R and T_g values of the EP's modified with HD-PUR-G and HD-PUR (cf. Table 2) one can state that the amine-functionality of HD-PUR-G and HD-PUR is comparable.

The theory of rubber elasticity was often used to correlate the fracture mechanical parameters with those of the cross-linked network [8,11–14]. According to this interpretation G_c shows a linear dependence when plotted as a function of $M_c^{1/2}$. Fig. 2 displays that the above
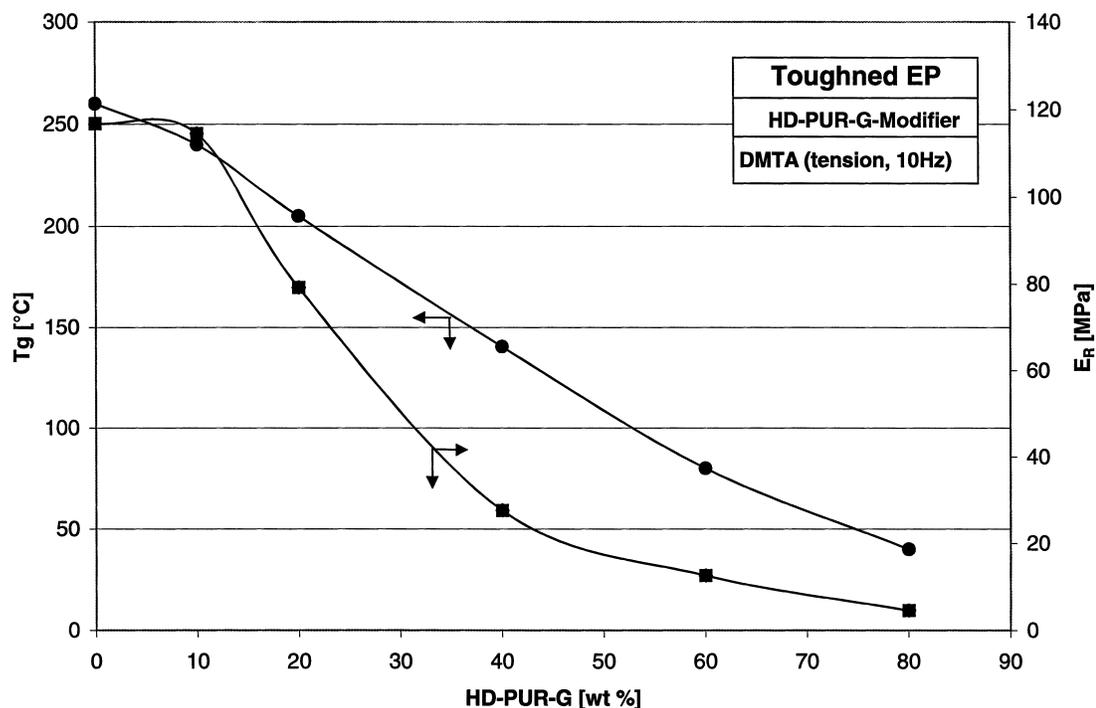
Fig. 1. Variation of T_g and E_R as a function of the HD-PUR-G amount added.
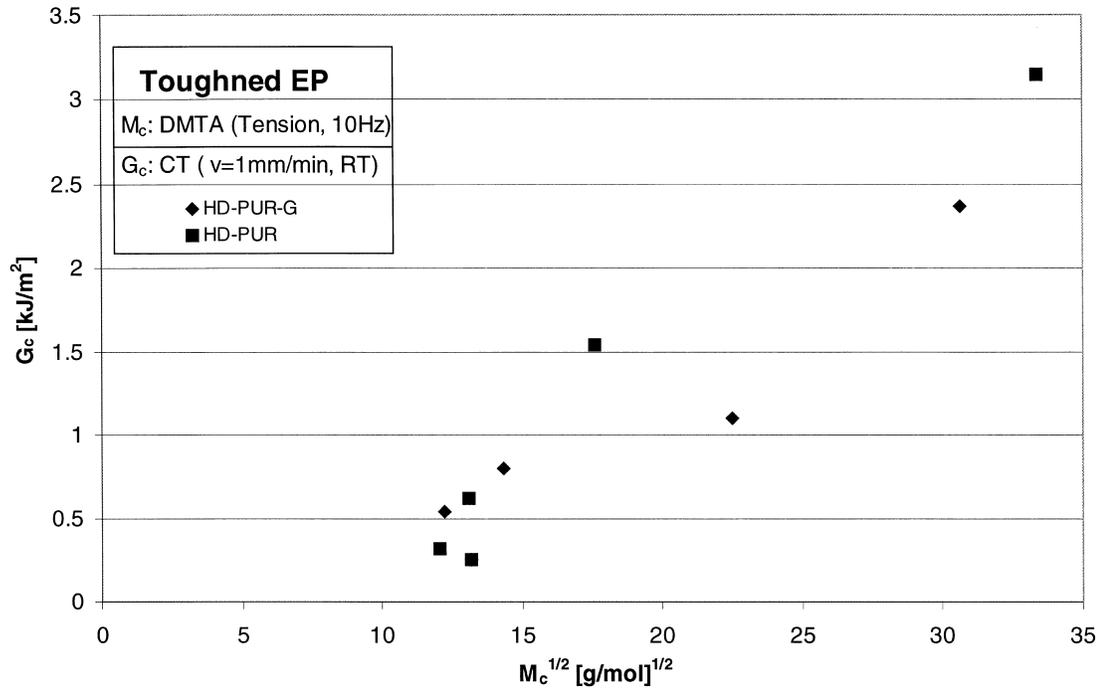
Fig. 2. Variation of fracture energy (G_c) as a function of $M_c^{1/2}$ for the EP systems modified with HD-PUR.

linear relationship holds also for our HD-PUR modified EP resins.

3.2. Solid particle erosion

3.2.1. Effects of modifier content and impact angle

The mass loss of the eroded specimens as a function of the modifier content and the impact angle is illustrated in Figs. 3 and 4 for the EPs modified by HD-PUR-G and HD-PUR, respectively. The curves in Figs. 3 and 4 show different courses upon the modifier content. The first learning from Figs. 3 and 4 is that the addition of HD-PUR results in systems with improved resistance to erosive wear. This improvement is, however, strongly dependent on the impact angle. The unmodified EP shows the largest weight loss at 60–90° impact angles. On the other hand, the EPs modified
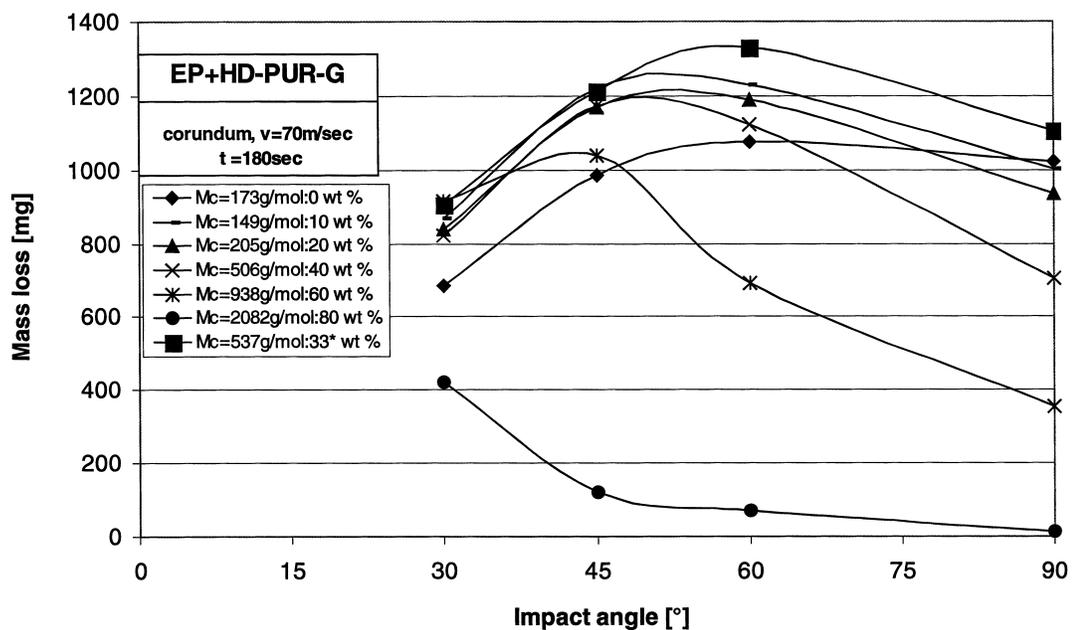
Fig. 3. Mass loss vs. impact angle traces for the EP systems modified with HD-PUR-G.
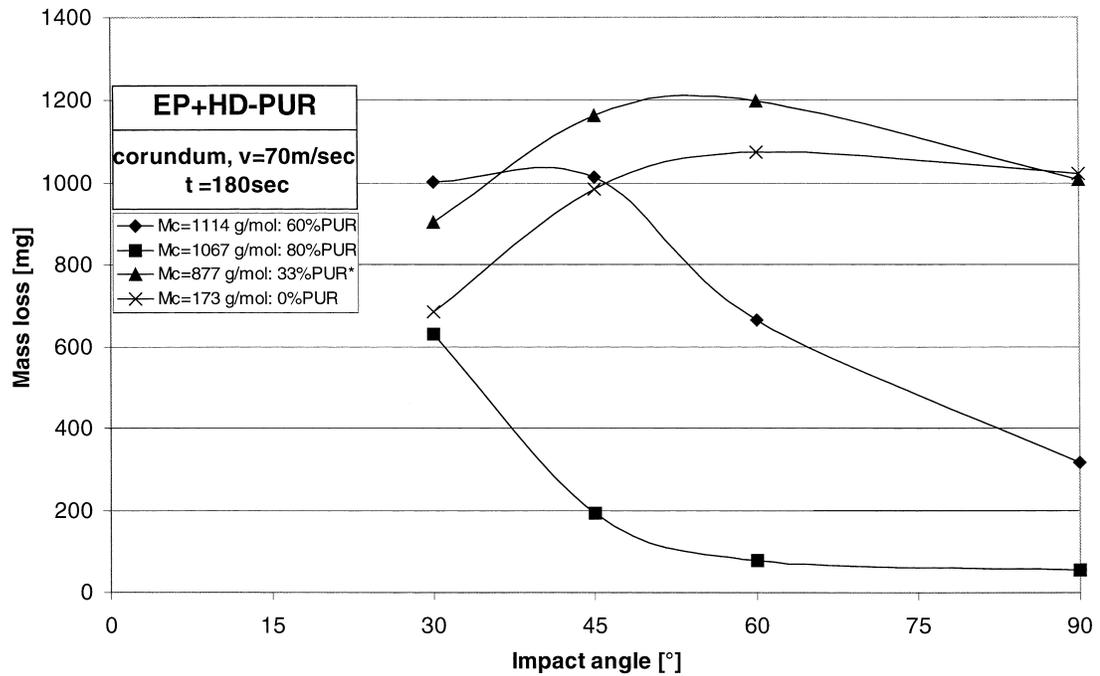
Fig. 4. Mass loss vs. impact angle traces for the EP systems modified with HD-PUR.

by 80 wt.% HD-PUR exhibit the highest erosion resistance in this range. One can recognise that EPs with less modifier than 40 wt.% show the highest erosion at 60°. The impact angle related to the maximum weight loss shifts to 30° when EPs containing more than 40 wt.% HD-PUR modifier are tested. Recall that such a shift should be associated with a change in the failure mode,

viz. from brittle via ductile to a rubbery-like failure mode.

3.2.2. Effects of mean molecular weight between cross-links (M_c)

Based on the M_c data indicated in Figs. 3 and 4 is obvious that the resistance to solid particle erosion at
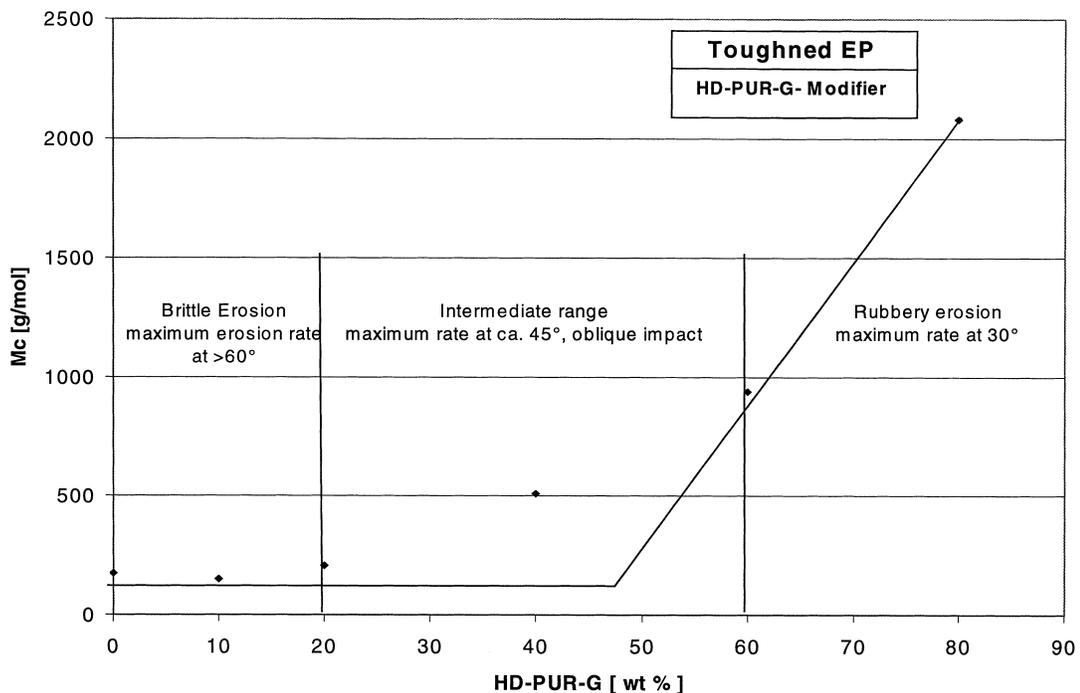
Fig. 5. Variation of M_c as a function of HD-PUR-G content. Note: this diagram indicates the maximum erosion rates and failure modes.
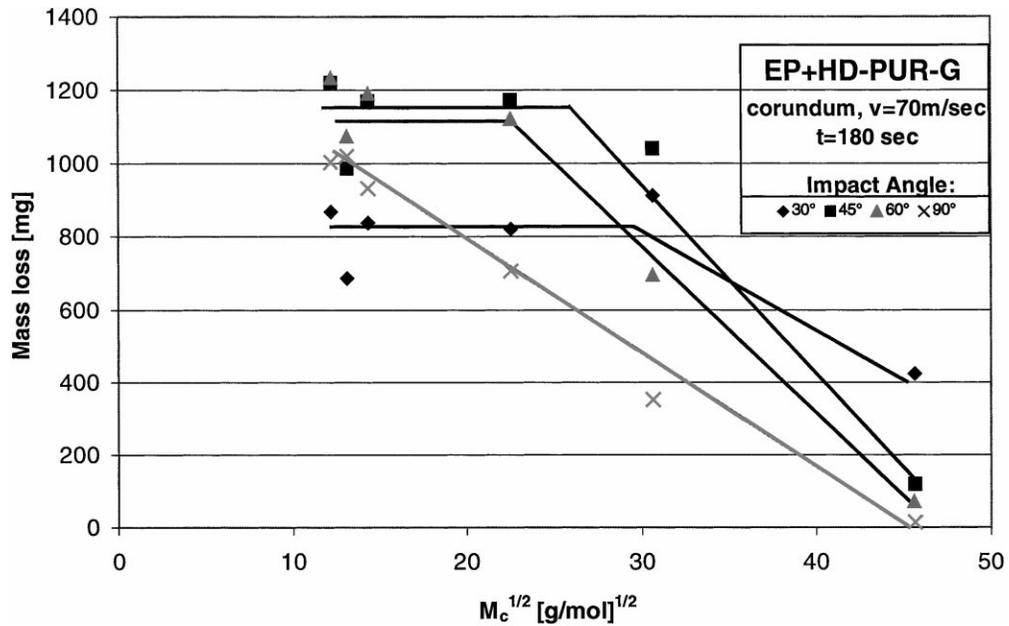
Fig. 6. Mass loss vs. $M_c^{1/2}$ diagram for EP/HD-PUR-G systems.

oblique angles strongly depends on the M_c value, or more generally, on characteristics of the cross-linked structure. Further, M_c seems to control whether the EP erodes in a brittle or rubbery-like manner. Fig. 5 suggests that the EP systems characterised by $M_c < 200$ g/mol fail brittely (as thermosets) whereas those having $M_c > 1000$ g/mol should show a rubbery-type erosion (as rubbers). These two extremes are separated by a rather large intermediate range

where the highest erosion rate can be found at about 45° impact angle.

The variation of the mass loss in function of M_c at oblique impact angles seems to start with a plateau followed by a steep decrease with increasing M_c. As the impact angle is increasing from 30 to 90°, this plateau becomes progressively smaller and even disappears at 90° impact (cf. Fig. 6). The physical interpretation of the findings presented in Fig. 6 is
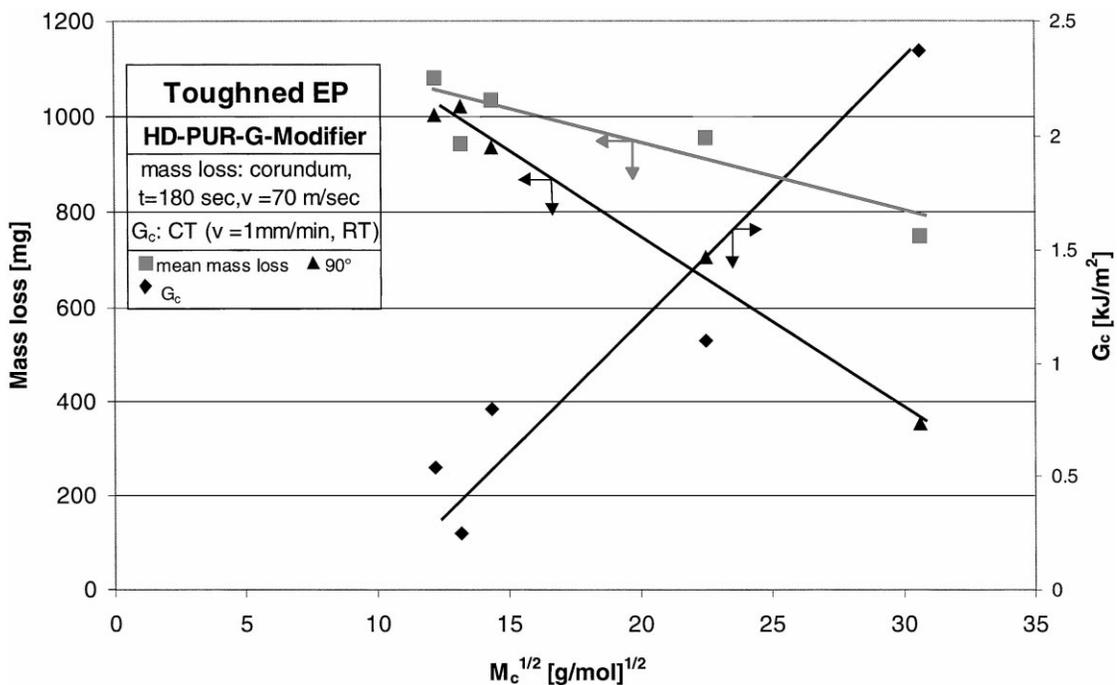
Fig. 7. Mass loss and fracture energy (G_c) vs. $M_c^{1/2}$ for the EP/HD-PUR-G systems.
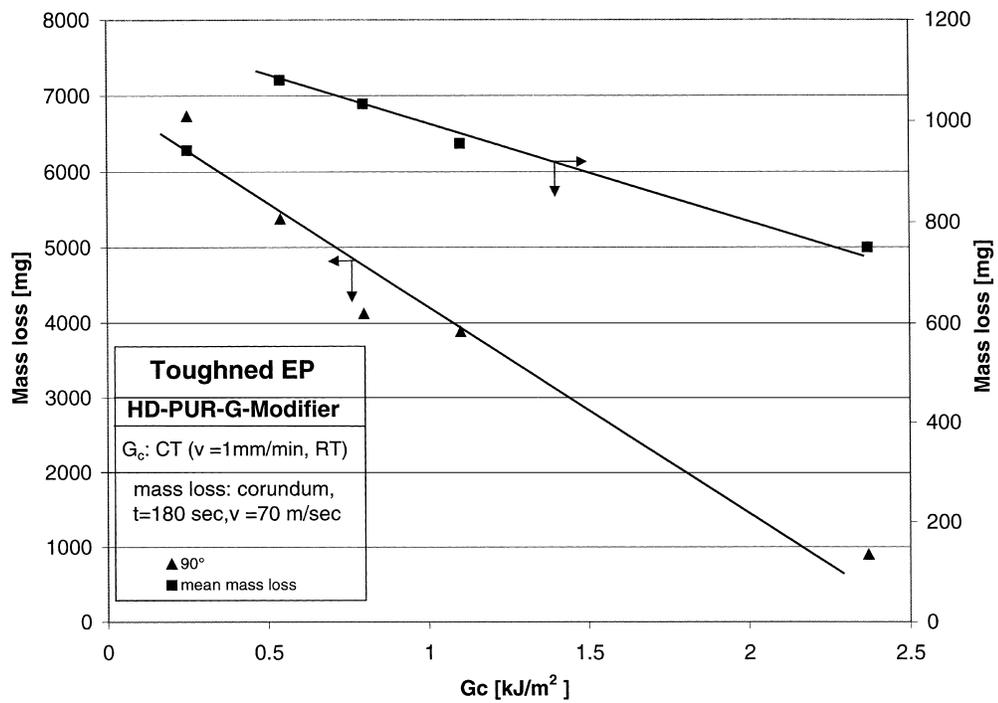
Fig. 8. Variation of mass loss as a function of G_c for the EP/HD-PUR-G compositions.
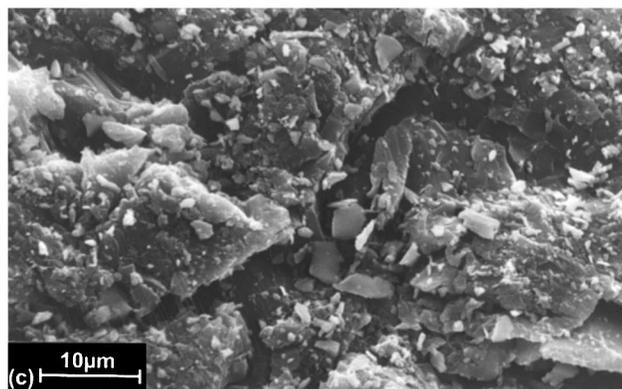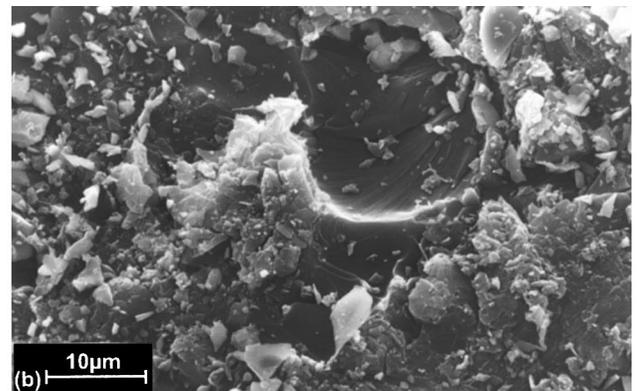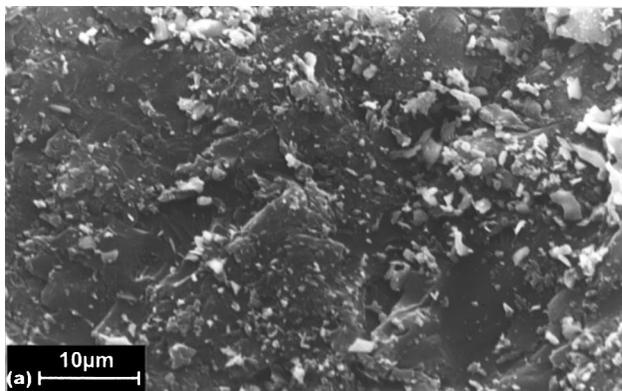
Fig. 9. Scanning electron micrographs taken on the eroded surface of pure EP after impact at (a) 30, (b) 60 and (c) 90° angles, respectively. Notes: erosion time: 180 s; erosion direction from left to right.

not easy as M_c is a direction independent material property. One could speculate, however, that the strong dependence of the maximum erosion on the impact angle is related to a change in the local loading mode. Under transverse impact (90°) mode I (crack opening), whereas at 30° oblique impact mode III (out-of-plane shear) conditions are likely dominating.

3.2.3. Correlation between erosion resistance and fracture energy

Fig. 7 depicts the mass loss and fracture energy (G_c) as a function of $M_c^{1/2}$. This figure shows the mass loss at 90° along with an impact angle-average value, denoted as mean mass loss. The latter is an arithmetic average of the erosion data determined at 30, 45, 60, and 90° particle impact. One can see that the erosion resistance linearly increases (or the erosion rate decreases) with increasing $M_c^{1/2}$. Figs. 2 and 7 also demonstrate that G_c increases linearly with $M_c^{1/2}$ as expected by considering the rubber elasticity theory. As a consequence, the increasing resistance to erosion is due to the increment in G_c. Fig. 8 displays that the mass loss changes inversely with G_c in fact.

3.2.4. Erosion mechanisms

As mentioned above the erosion failure mechanisms can be grouped into brittle, ductile and rubbery ones. The observed dependence of the erosive wear on the impact angle for the modified EPs of various cross-linked networks suggests that the erosion mechanism depends on M_c. In highly cross-linked systems, characterised by low M_c values, brittle erosion should dominate. Characteristic SEM pictures taken on the surface of the unmodified EP samples eroded at various impact angles show a smooth surface at 30° (cf. Fig. 9a) and a very rough one at 60 and 90° (cf. Fig. 9b and c). A smooth surface means high, whereas a rough one low resistance to erosion in the first approximation. Fig. 9 also suggests that the temperature of the EP during jet erosion did not reach the T_g and, thus the EP failed in a highly brittle manner. A similar failure scenario holds for samples with less than ca. 20 wt.% HD-PUR-G modifier. By contrast, the EP with 80 wt.% HD-PUR-G shows a more rough surface after particle impact at 30° (cf. Fig. 10a) than at 60 or 90° (cf. Fig. 10b and c). Further, Fig. 10a evidences that rubbery-like failure occurred. The appearance of the eroded surface hints that the T_g of this composition was surpassed due to the erodent flux. The related heat softening in combination with the lower hardness (cf. Table 2) of the systems with high amount of modifier, explains also why an incubation period, mentioned above was observed. Note that ductile and rubbery materials present a better resistance to erosion for all impact angles and they need more impact time to erode in comparison
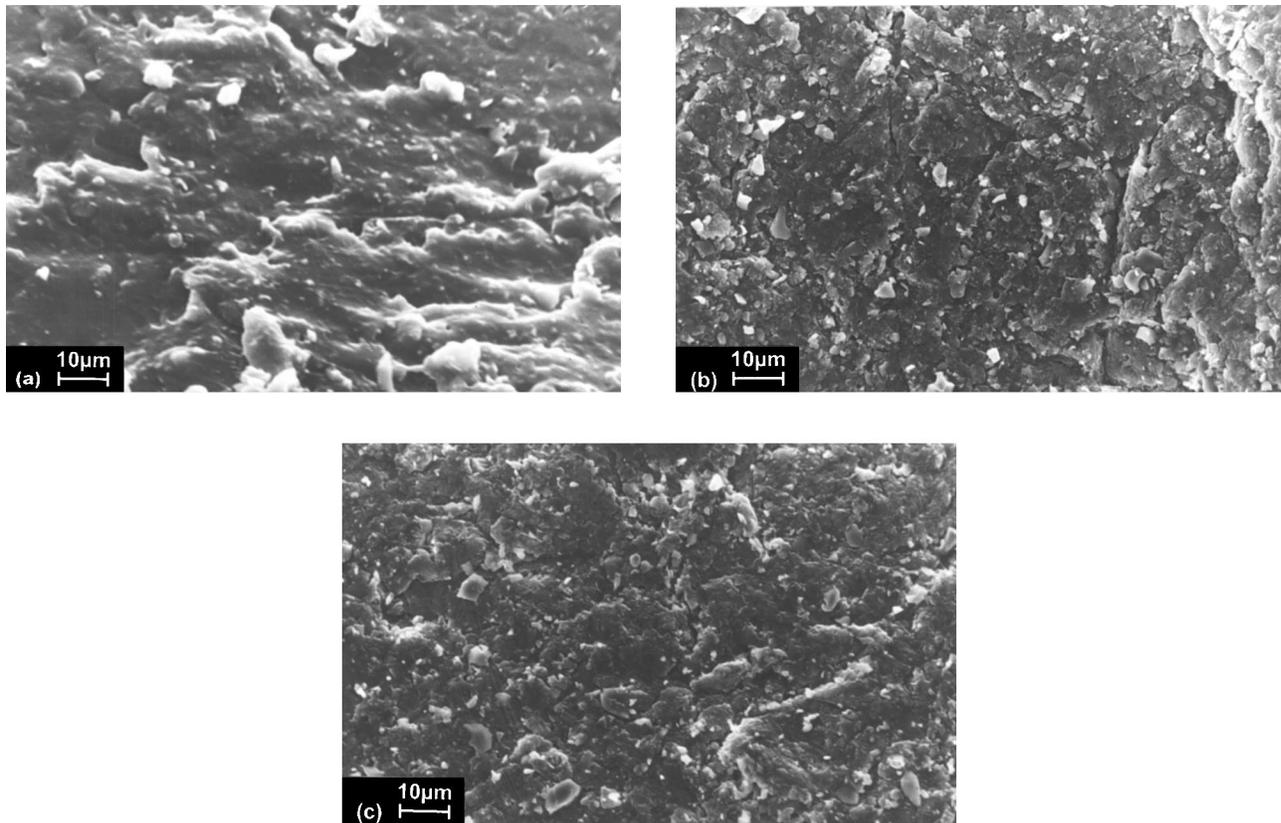
Fig. 10. Scanning electron micrographs taken on the eroded surface of EP/HD-PUR-G system containing 80 wt.% HD-PUR-G after impact at (a) 30, (b) 60 and (c) 90° angles, respectively. Erosion time: 180 s; erosion direction from left to right.

to brittle ones. Therefore, the existence of the incubation period is also a proof of better erosion resistance. Note that during the incubation period substantial amount of impact energy is dissipated in roughening the target surface. An incubation period was observed for the case of EP with 80 wt.% HD-PUR-G at 60 and 90° impact angles, where the mass loss was the lowest (cf. Fig. 3).

It is already known that the impact angle is one of the important parameters in respect to the erosion behaviour. When the erosive particles hit the target at low angles, the impact force can be divided into two constituents. One is parallel (F_p) to the surface of the material and the other is vertical (F_v). F_p controls the abrasive and F_v is responsible for the impact phenomena. As the impact angle is shifting towards 90°, the effects of F_p become marginal. It is obvious, that in the case of normal erosion all available energy is dissipated by impact and microcracking, while at oblique angles due to the decisive role of the F_p the damage occurs by microcutting and microploughing [15,16]. This is not the case for elastomers, where in both oblique and normal impact the material removal takes place by fatigue crack propagation. At high impact angles the wear mechanism in erosion involves the propagation of fatigue cracks under the influence of frictional stresses arising from particle impact [17]. At low angles the erosion may proceed by a catastrophic tearing process which shows many similarities to that occurring during sliding abrasion by a blade or by a smooth indentor [18]. Ploughing features characteristic for ductile type of erosion in case of thermoplastics could not be resolved. The failure in Fig. 10a and b seems to support the analogy between the EP modified by high amount of HD-PUR-G and elastomers. That is the reason why the term "rubbery failure" has been used throughout the text.

4. Conclusions

Based on this study performed on the solid particle erosion of modified EP resins having different cross-linking density, the following conclusions can be drawn:

- The erosion behaviour depends on both external (impact angle) and internal (mean molecular weight between cross-links, M_c) parameters. Compositions of low M_c showed the lowest resistance at normal impact and failed brittly, whereas those of high M_c had the lowest erosion at oblique impact of 30° and failed by fatigue crack growth.
- Impact modification of EP by hygrothermally decomposed polyester-urethane (HD-PUR) resulted in improved fracture energy (G_c) and increased the overall resistance to solid particle erosion, as well.
- Linear correlation was concluded between the resistance to erosion and G_c. The latter correlated with $M_c^{1/2}$,

corroborating the validity of the rubber elasticity theory for the modified EPs studied.

References

[1] A. Häger, K. Friedrich, Y. Dzenis, S.A. Paipetis, Study of erosion wear of advanced polymer composites, in: K. Street, B.C. Whistler (Eds.), Proceedings of the ICCM-10, Canada, Woodhead Publishing Ltd., Cambridge, UK, 1995, pp. 155–162.

[2] G.P. Tilly, W. Sage, The interaction of particle and material behaviour in erosion process, Wear 16 (1970) 447–465.

[3] M. Roy, B. Vishwanathan, G. Sundararajan, The solid particle erosion of polymer matrix composites, Wear 171 (1994) 149–161.

[4] I. Finnie, Some reflections on the past and future of erosion, Wear 186/187 (1995) 1–10.

[5] I. Finnie, G.R. Stevick, J.R. Ridgely, The influence of impingement angle on the erosion of ductile metals by angular abrasive particles, Wear 152 (1992) 91–98.

[6] P. Chevallier, A.B. Vannes, Effect on a sheet surface of an erosive particle jet upon impact, Wear 184 (1995) 87–91.

[7] W. Tabakoff, High-temperature erosion resistance of coatings for use in turbomachinery, Wear 186/187 (1995) 224–229.

[8] J. Karger-Kocsis, J. Gremmels, Use of hygrothermal decomposed polyester-urethane waste for the impact modification of epoxy resins, J. Appl. Polym. Sci. 78 (2000) 1139–1151.

[9] J. Karger-Kocsis, J. Gremmels, Toughening of epoxy resins by partially decomposed polyurethane waste, SPE-ANTEC 46 (2000) 840–844.

[10] ESIS-TC4, A linear elastic fracture mechanics (LEFM) standard for determination K_c and G_c for plastics, Testing Protocol, March 1990.

[11] T. Iijima, N. Yoshioka, M. Tomoi, Effect of cross-link density on modification of epoxy resins with reactive acrylic elastomers, Eur. Polym. J. 28 (1992) 573–581.

[12] E. Urbaczewski-Espuche, J. Galy, J.-F. Gerard, J.-P. Pascault, H. Sautereau, Influence of chain flexibility and cross-link density on mechanical properties of epoxy/amine networks, Polym. Eng. Sci. 31 (1991) 1572–1580.

[13] R.A. Pearson, A.F. Yee, Toughening mechanisms in elastomer-modified epoxies, J. Mater. Sci. 24 (1989) 2571–2580.

[14] M.C. Shaw, E. Young, Rubber elasticity and fracture, J. Eng. Mater. Technol. 110 (1988) 258–265.

[15] K. Friedrich, Erosive wear of polymer surfaces by steel ball blasting, J. Mater. Sci. 21 (1986) 3317–3332.

[16] Y.Q. Wang, L.P. Huang, W.L. Liu, J. Li, The blast erosion behaviour of ultrahigh molecular weight polyethylene, Wear 218 (1998) 128–133.

[17] J.C. Arnold, I.M. Hutchings, Erosive wear of rubber by solid particles at normal incidence, Wear 161 (1993) 213–221.

[18] J.C. Arnold, I.M. Hutchings, A model for the erosive wear of rubber at oblique impact angles, J. Phys. D: Appl. Phys. 25 (1992) A222–229.